CHEMISTRY
A European Journal

A Journal of
ChemPubSoc Europe

Accepted Article

Title: Selective Photooxidation of Sulphides catalyzed by Biscyclometalated IrIII Photosensitizers Bearing 2,2'-dipyridylamine Based Ligands

Authors: Mónica Vaquero, Alba Ruiz-Riaguas, Marta Martínez-Alonso, Félix Ángel Jalón, Blanca Rosa Manzano, Ana María Rodríguez, Gabriel García-Herbosa, Carbayo Aránzazu, Begoña García, and Gustavo Espino

To be cited as: *Chem. Eur. J.* 10.1002/chem.201801173

Link to VoR: http://dx.doi.org/10.1002/chem.201801173

Supported by
ACES

WILEY-VCH

10.1002/chem.201801173

WILEY-VCH

Selective Photooxidation of Sulphides catalyzed by Biscyclometalated Ir^{III} Photosensitizers Bearing 2,2'-dipyridylamine Based Ligands

Mónica Vaquero,*[a] Alba Ruiz-Riaguas,[a] Marta Martínez-Alonso,[a] Félix A. Jalón,[b] Blanca R. Manzano,[b] Ana M. Rodríguez,[b] Gabriel García-Herbosa,[a] Arancha Carbayo,[a] Begoña García,[a] Gustavo Espino.*[a]

Abstract: A new family of heteroleptic biscyclometalated Ir^{III} complexes with formula $[Ir(C^N)_2(N^N)]Cl$, where (C^N) = 2-phenylpyridinate and (N^N) = 2,2'-dipyridylamine or N-benzylated-2,2'-dipyridylamine, have been synthesized, characterized and successfully used as photosensitizers in the catalytic photooxidation of an array of dialkyl, dibenzyl, alkylaryl and diaryl sulphides, as well as sulphur-containing aminoacids. Furthermore, the reactions proceeded with optimal chemo-selectivity and atom economy under smooth conditions. Experimental observations support a dual mechanism where singlet oxygen and superoxide are the actual oxidants.

Introduction

Photocatalysis is becoming a very useful and environmentally benign strategy in organic synthesis, since it allows transforming a variety of substrates using mild conditions and light as the source of energy instead of heat.[1–3] Specifically, aerobic photooxidation utilizes plentiful and harmless O_2 as the oxidant agent rather than expensive, toxic or corrosive oxidants adopted in traditional oxidation processes. This approach involves the use of a photosensitizer (PS) or photocatalyst which is excited through irradiation with light, in such a way that in the presence of O_2, it can generate highly reactive oxygen species (ROS), namely singlet oxygen ($^1O_2$) or superoxide radical ($O_2^{\bullet-}$) by mean of an energy transfer process (ET) or an electron transfer reaction (eT), respectively.[4] Ultimately, these oxygen species execute the oxidation of the organic substrates and biomolecules. The ideal PSs for catalytic photooxidation should conjugate the following features:[5] (a) broad overlapping between the absorption spectra of the PS and the emission band of the light source (visible light preferably) together with high molar extinction coefficients; (b) high intersystem crossing efficiency to guarantee high quantum yields in the formation of the PS triplet excited state; (c) long triplet excited state lifetimes and good quantum yields in the generation of singlet oxygen ($^1O_2$) or alternatively superoxide radical ($O_2^{\bullet-}$) in the chosen solvent; and (d) high solubility and photostability in the solvent used for the reaction.

The group of traditional $^1O_2$ photosensitizers comprises different families of organic compounds such as porphyrins, phthalocyanines, fullerene derivatives and organic dyes (e.g. Rose Bengal, Methylene Blue), but most of them undergo degradation upon irradiation and cannot be easily modified in order to modulate their photophysical properties. On the contrary, Ru^{II} polypyridyl complexes and Ir^{III} biscyclometallated compounds have proved to combine efficient $^1O_2$ (or $O_2^{\bullet-}$) photosensitizing abilities or photoredox catalytic activity along with a good photostability and a modular structure which can be readily modified,[6,7] and are emerging as ideal candidates to be used as PSs in the photocatalytic oxidation of organic substrates and biomolecules.[8]

Sulfoxides are very important intermediates in organic synthesis, and some of them are commercialized as drugs owing to their pharmacological activity,[2,9,10] e.g. alliin, armodafinil and esomeprazole.[11] Hence, the development of chemo-selective and efficient methods of synthesis from the respective sulphides is an appealing challenge.[12,13] Previously, aerobic photooxidation of sulphides has been successfully accomplished using either metal complexes or organic dyes as PSs. In particular, it is worth mentioning the systems reported recently using photosensitizers based on tetra-O-acetyl-riboflavine,[2,9] Rose Begal,[14] Thioxanthones,[15] Pt^{II} complexes[16], Ru^{II}-Cu^{II} complexes,[17] coenzyme NAD^+[18] and BODIPY dyes.[19] However, as far as we know, Ir^{III} complexes have not been used in similar studies and what is more, improvements can still be made in the field to shorten reaction times, enhance the photostability and the recyclability of PSs, optimize the selectivity of the reaction, expand the substrate scope, and avoid organic solvents and UV light.

In this work, we disclose for the first time the broad applicability of a new family of biscyclometallated Ir^{III} complexes with N^N ancillary ligands based on the 2,2'-dipyridylamine scaffold (**L1**) as PSs for the selective aerobic photooxidation of organic sulphides and sulfur containing *L*-aminoacids. In addition, we assess the effect of functionalizing the N-H group of **L1** with different benzyl moieties over their photophysical properties, their photostability and their activity in the above-mentioned photocatalytic reaction.

[a] Dr. M. Vaquero, A. Ruiz-Riaguas, Dr. M. Martínez-Alonso, Dr. García-Herbosa, Dr. A. Carbayo, Dr. B. García, Dr. G. Espino.
Departamento de Química, Facultad de Ciencias
Universidad de Burgos
Plaza Misael Bañuelos s/n, 09001, Burgos, Spain
E-mail: mvaquero@ubu.es
E-mail: gespino@ubu.es

[b] Dr. F A. Jalón, Dr. B.R. Manzano, Dr. A. M. Rodríguez
Departamento de Química Inorgánica, Orgánica y Bioquímica,
Facultad de Químicas
Universidad de Castilla-La Mancha
Avda. Camilo J. Cela 10, 13071 Ciudad Real, Spain

Supporting information for this article is given via a link at the end of the document.

Results and Discussion

1.- Synthesis and characterization of ligands (L1-L4) and Ir^{III} complexes ([1]Cl-[4]Cl)

Ligands: Ligand **L1** (2,2'-dipyridylamine) is commercially available, and ligands **L2-L4** were prepared by reacting **L1** with the appropriate benzyl bromide in the presence of KOH to deprotonate the N-H group and using DMSO as the solvent at room temperature (see Scheme 1). This procedure has been adapted and optimized from those reported in the literature.[20–24]

Cyclometalated Ir^{III} complexes. The new Ir^{III} compounds **[1]Cl-[4]Cl** of general formula $[Ir(C^N)_2(N^N)]Cl$ (C^N = 2-phenylpyridinate (ppy^-), N^N = **L1-L4**) were synthesized according to the classical procedure,[25] which involves two steps: preparation of the well-known chloro-bridged dimer $[Ir(\mu\text{-}Cl)(C^N)_2]_2$, followed by its reaction with the corresponding N^N ligand in a mixture of CH_2Cl_2/MeOH at 50 °C as sketched in Scheme 2. The desired compounds were obtained in good yields as the chloride salts of the Ir^{III} cationic complexes in the form of racemic mixtures (Λ and Δ enantiomers). Moreover, they are air- and moisture-stable yellow solids, soluble in common organic solvents. Complex **[1]$^+$** has been described previously in the form of the PF_6^- salt,[26] but the synthesis and characterization of the Cl^- salt had not been reported so far.

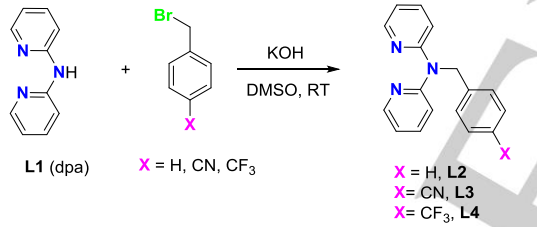

Scheme 1. Reaction protocol for the synthesis of ancillary ligands **L2-L4**.

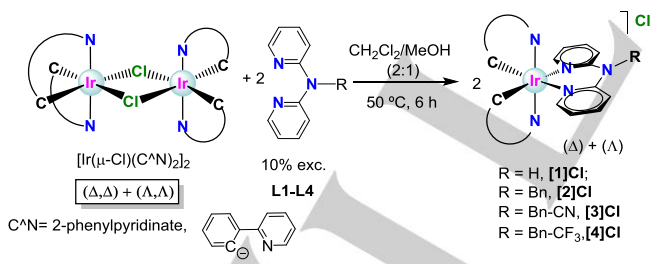

Scheme 2. Reaction protocol for the synthesis of complexes **[1]Cl-[4]Cl** (Bn = benzyl).

2. Characterization of Ir^{III} complexes [1]Cl-[4]Cl in solution

All the compounds synthesized in this work have been fully characterized by NMR, HR-ESI Mass and IR spectroscopy, as well as by elemental analysis. In addition, the structure of complex **[1]Cl** has been confirmed by X-ray diffraction.

The ^1H NMR spectra of the above-mentioned ligands and complexes were recorded in $[D_6]$DMSO at 25 °C and 2D-COSY and 2D-NOESY experiments were carried out to assign all the resonances. Atom labelling, and comparative tables of chemical shifts are provided in SI (Table SI1 and SI2). The following general features are deduced from the spectra of the new complexes:

a) A single set of 8 resonances (each integrating as 2 H) is observed for the two C^N ligands due to the symmetric nature of these complexes (C_2-symmetry).

b) A single set of 4 resonances is recorded for the two pyridyl rings of the N^N ligands owing to their symmetry equivalence.

c) Two geminally coupled doublets at around 5.2 and 5.7 ppm (1 H each) are observed for the diastereotopic protons of the methylene group in complexes **[2]Cl-[4]Cl**, whereas a singlet (2 H) is observed for the homotopic protons of the -CH_2 groups in the respective free ligands. This symptomatic change after coordination is the result of the chirality inherent to tris-chelate octahedral complexes.

d) A strongly deshielded singlet is observed at 11.09 ppm for the N-H group of complex **[1]Cl**.

e) In general, the pyridine protons of the N^N ligand undergo a shift to lower field with respect to the free ligand.

The $^{19}F\{^1H\}$ NMR spectrum of **[4]Cl** exhibits a singlet at -60.9 ppm for the –CF_3 group.

The high resolution HR-ESI(+) mass spectra recorded for the new complexes **[1]Cl-[4]Cl**, exhibited in every case a parent peak envelope, whose *m/z* ratio and isotopic pattern are fully compatible with cationic fragments of formulae $[Ir(C^N)_2(N^N)]^+$. Moreover, the spectrum of **[1]Cl** features a second peak envelope attributable to the fragment $[Ir(C^N)_2]^+$, owing to the loss of **L1** (see Figure SI1).[27]

3. Crystal Structure by X-ray Diffraction

Single crystals of **[1]Cl**·CH_2Cl_2·0.25H_2O suitable for X-ray diffraction analysis were obtained by slow evaporation of a solution of **[1]Cl** in dichloromethane. Complex **[1]Cl**·CH_2Cl_2·0.25H_2O crystallizes in the monoclinic space group $P2_1/c$. The ORTEP diagram for (Δ)-**[1]Cl** is depicted in Figure 1, selected bond lengths and angles with estimated standard deviations are gathered in Table 1, and crystallographic refinement parameters are given in the Supporting Information (Table SI3). The corresponding unit cell shows two pairs of the enantiomers (Λ) and (Δ) stemming from helical chirality implicit in trischelate octahedral metal complexes. Furthermore, the unit cell contains four Cl^- counterions plus four molecules of CH_2Cl_2 and one molecule of H_2O. The CH_2Cl_2 molecules display positional disorder and the proton atoms of H_2O have not been localized. The iridium center displays a slightly distorted octahedral coordination geometry with the expected *cis*-C,C and *trans*-N,N mutual disposition for the C^N ligands.

The bond lengths and angles are very similar to those reported for the PF_6^- salt (see Table 1).[26] In particular, the Ir-C_{ppy} and Ir-N_{ppy} bond distances lie in the expected ranges for 2-phenylpyridinate ligands, that is, very close to 2 Å.[26,28–33] The bond lengths for the ancillary ligand are significantly longer due

to the strong *trans* influence attributed to the C atoms of the C^N ligands, Ir(1)-N(3) = 2.177(4) Å and Ir(1)-N(4) = 2.166(4) Å.[34,35]

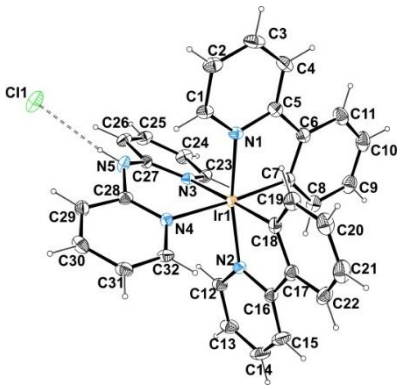

Figure 1: ORTEP diagram for (Δ)-**[1]Cl** forming part of the asymmetric unit of racemic **[1]Cl**·CH_2Cl_2·0.25H_2O. Thermal ellipsoids are shown at the 30% probability level. The CH_2Cl_2 and H_2O molecules have been omitted for the sake of clarity.

Table 1. Selected bond lengths (Å) and angles (°) for the crystal structure of **[1]Cl**·CH_2Cl_2·0.25H_2O and **[1]PF_6**·$(CH_2Cl_2)_2$[a][26]

Distances	[1]Cl	[1]PF_6	Angles	[1]Cl	[1]PF_6
Ir(1)-N(1)	2.054(4)	2.049(6)	C(7)-Ir(1)-N(1)	80.20(19)	80.1(4)
Ir(1)-N(2)	2.040(4)	2.037(6)	C(18)-Ir(1)-N(2)	80.51(19)	80.5(3)
Ir(1)-N(3)	2.177(4)	2.173(6)	N(4)-Ir(1)-N(3)	86.44(15)	86.0(2)
Ir(1)-N(4)	2.166(4)	2.168(6)	N(2)-Ir(1)-N(1)	169.85(16)	172.7(2)
Ir(1)-C(7)	2.006(5)	2.010(7)	C(7)-Ir(1)-N(4)	176.34(17)	176.7(3)
Ir(1)-C(18)	2.004(5)	2.008(7)	C(18)-Ir(1)-N(3)	177.73(18)	177.0(3)

[a]Data for **[1]PF_6** have been taken from the literature[26] and are shown for comparison.

The bite angle for the N^N ligand, N(4)-Ir(1)-N(3) = 86.44(15)°, is comparable to those previously reported for six-membered N-Ir-N iridacycles in analogous derivatives, and the C-Ir-N bite angles for the ppy$^-$ ligands, C(7)-Ir(1)-N(1) and C(18)-Ir(1)-N(2), are also standard (80.20(19)° and 80.51(19)°, respectively).[32,36,37] Moreover, the C^N chelate rings are essentially planar, whereas the N^N chelate ring exhibits a boat conformation. The 3D crystal packing is hold down by intermolecular hydrogen bonds (with the participation of the cations, the solvent molecules and the Cl^- anion), CH-π contacts and offset π–π stacking interactions. It is worth remarking the pivotal cohesive role exerted by the Cl^- counterion, that takes part in five hydrogen bonding contacts (NH···Cl^- or CH···Cl^-) as an acceptor involving three different units of **[1]**$^+$ and a CH_2Cl_2 molecule as donors (see Table SI4 and Figure SI2). Columns of π–π stacking interactions that extend along *c* axis are formed involving alternate phenyl and pyridine rings of the same cyclometalating ligand (see Figure SI3 and Table SI5).

In addition, a remarkable motif in this structure is formed by pairs of complex cations interacting through a parallel four-fold pyridyl embrace[38] which involves an offset π–π stacking interaction and two CH–π contacts (see Figure SI4 and Table SI5). Two pyridine rings of each cation (one of a ppy$^-$ ligand and another from the N^N ligand) take part in this embrace. This is a particular case of the more general term multiple aryl embrace, a "synthon" that is receiving increasing attention in the field of supramolecular chemistry.[39]

4. Photophysical properties

4.1. Electronic absorption properties. The UV-vis absorption spectra of ligands **L1-L4** (see Figure SI5, and data in Table SI6) and complexes **[1]Cl-[4]Cl** (see Figure 2, data in Table 2) were recorded in acetonitrile solutions (10^{-5} M) at 25 °C.

The spectra of complexes **[1]Cl-[4]Cl** feature two intense absorption bands between 190 and 330 nm, which are attributed to singlet spin-allowed ligand centered (^{1}LC) transitions taking place in both the N^N and the N^C ligands. Very weak and unstructured bands are also observed from 330 nm to 440 or 450 nm approximately (see Figure 2 and Table 2). These bands are assigned to spin-allowed ^{1}MLCT and spin-forbidden ^{3}MLCT (singlet to triplet $d\pi(Ir) \rightarrow \pi*(N^N)$), ^{3}LLCT (singlet to triplet, $3\pi(N^N) \rightarrow \pi^*(C^N)$) and ^{3}LC (singlet to triplet $3\pi \rightarrow \pi*$) transitions.[27]

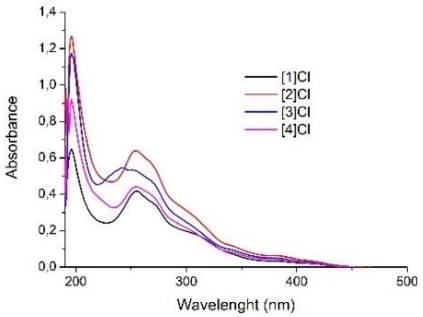

Figure 2. UV-vis absorption spectra of **[1]Cl-[4]Cl** (10^{-5} M) in acetonitrile at 25 °C

Taking into account that most of the photocatalytic experiments have been done in a mixture of DMSO/H_2O (3:2) (vide infra), the absorption spectra of complexes **[1]Cl-[4]Cl** (10^{-5} M) were also recorded in this solvent system at 25 ºC (see Figure SI7). Thus, we proved that the absorption spectra of our PSs and the emission spectrum of the blue light used in the photooxidation assays partially overlap one to another and hence we conclude that excitation of our PSs is feasible under this light source (λ = 460 nm) (see Figure SI8). Furthermore, no important solvatochromic effects were observed when comparing the spectra in both solvent systems (compare Table 2 and Table SI7).

Table 2. Wavelengths (λ_{abs}) and molar extinction coefficients (ε) at the absorption maxima and relative maxima in the UV-vis spectra of complexes **[1]Cl-[4]Cl** measured in acetonitrile at 25 °C.

Complex	λ_{abs} [nm]	ε [10^3 M^{-1} cm^{-1}]
[1]Cl	196, 255, 386	64.8, 41.7, 3.3
[2]Cl	196, 254, 386	126.8, 63.8, 6.1
[3]Cl	196, 254, 342	117.3, 53.1, 9.2
[4]Cl	196, 255, 343	92.1, 43.9, 7.8

4.2. Photoluminescence properties

The complexes **[1]Cl-[4]Cl** show photoluminescence in the cyan hue under irradiation with UV light. The respective emission spectra were recorded for 10^{-5} M solutions in dry and deoxygenated acetonitrile at 25 °C (see Figure 3 and Table 3). All the spectra are very similar and show a broad band with two maxima at 478 and 508 nm, and a shoulder around 550 nm, revealing the negligible effect that substitution of the N-H group with different benzyl groups exerts on the emitting excited states. Phosphorescent emission in complexes of the type $[Ir(C^N)_2(N^N)]^+$ takes place from the lowest-lying triplet state (T_1), which usually is made up from a combination of metal-to-ligand and ligand-to-ligand charge transfer (^{3}MLCT and ^{3}LLCT, respectively) and ligand-centered (^{3}LC) triplet states.[40] Nevertheless, the structured form of the bands recorded for our complexes points out to a dominant ^{3}LC nature of the transitions.[27] As for the quantum yields, ϕ_{PL}, complex **[1]Cl** exhibits the highest value (45.1 %), whereas the benzyl derivatives undergo a significant drop in the quantum efficiency below 5% (4.3-4.9 %) (see Table 3 and Figure SI9).

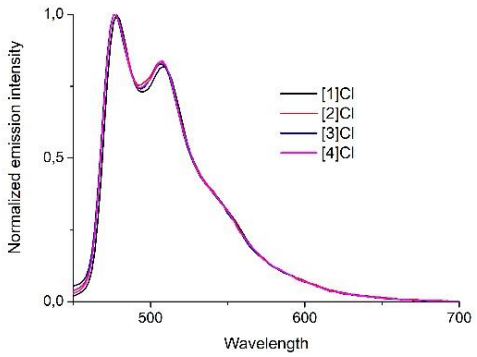

Figure 3. Emission spectra of complexes of **[1]Cl-[4]Cl** in acetonitrile (10^{-5} M) at 25 °C.

Moreover, the emission spectra and photophysical properties were also recorded for **[1]Cl** and **[3]Cl** in the mixtures of solvents used in the photocatalytic experiments, namely, deoxygenated DMSO/H_2O (3:2) and [D_6]DMSO/D_2O (3:2) (see Figure SI10 and Table 4). Although, solvatochromic effects on the emission wavelengths were insignificant, the half-life times ($\tau_{1/2}$) of **[1]Cl** and **[3]Cl** are considerably enhanced in compariso to those for acetonitrile solutions, suggesting that the presence of polar protic solvents could stabilize the excited state, in agreement with a non-negligible contribution of polar charge transfer (CT) states to the triplet, T_1, which is mainly LC in nature.[41] In particular, the $\tau_{1/2}$ values recorded in DMSO/H_2O and [D_6]DMSO/D_2O were 1365 and 1356 ns, respectively.

Table 3. Photophysical data for complexes **[1]Cl-[4]Cl** (10^{-5} M) in deoxygenated acetonitrile at 25 °C.

Complex	λ_{em} [nm][a]	$\Delta\lambda$ [nm][b]	ϕ_{PL} [%][c]	$\tau_{1/2}$ [ns][d]
[1]Cl	480, 510	170, 200	45.07	256.4
[2]Cl	478, 508	168, 198	4.46	208.0
[3]Cl	478, 508	168, 198	4.33	264.0
[4]Cl	478, 508	168. 198	4.94	470.1

[a] λ_{em} were recorded with λ_{exc} = 310 nm [b] $\Delta\lambda$: Stokes Shift. [c] Quantum Yields were recorded with λ_{exc} = 405 nm [d] $\tau_{1/2}$ were recorded with λ_{exc} = 375 nm.

Regarding the photoluminescence quantum yield (ϕ_{PL}), both complexes, **[1]Cl** and **[3]Cl**, exhibited better emission efficiencies in DMSO/H_2O (3:2) than in CH_3CN. This is particularly remarkable in the case of **[3]Cl** and is likely related to the higher photostability of this complex in DMSO/H_2O (vide infra). In the mixture [D_6]DMSO/D_2O (3:2) the emission is also efficient and shows ϕ_{PL} values above 40%.

Table 4. Photophysical data for complexes **[1]Cl** and **[3]Cl** (10^{-5} M) in DMSO/H_2O (3:2) and [D_6]DMSO/D_2O (3:2) at 25 °C.

Ir^{III} PS (solvent)	λ_{em} [nm][a]	$\Delta\lambda$ [nm][b]	ϕ_{PL} [%][c]	$\tau_{1/2}$ [ns][d]
[1]Cl (DMSO/H_2O)	480, 510	170, 200	65.21	1482.74
[1]Cl ([D_6]DMSO/D_2O)	480, 511	170, 201	45.37	1821.61
[3]Cl (DMSO/H_2O)	478, 508	168. 198	55.84	1365.08
[3]Cl ([D_6]DMSO/D_2O)	478, 508	168. 198	43.02	1356.08

[a] λ_{em} were recorded with λ_{exc} = 310 nm [b] $\Delta\lambda$: Stokes Shift. [c] Quantum Yields were recorded with λ_{exc} = 405 nm [d] $\tau_{1/2}$ were recorded with λ_{exc} = 375 nm.

5. Electrochemical behavior

The redox potentials of **[1]Cl-[4]Cl** and thioanisole were determined in degassed acetonitrile solutions by cyclic voltammetry (CV) using [^{n}Bu$_4$N][PF_6] as supporting electrolyte

and glassy carbon as the working electrode. Potentials are given with respect to the ferrocene/ferrocenium (Fc/Fc^+) couple (Figure SI11 and Table SI8). Thus, in the anodic region all the photosensitizers exhibit an irreversible oxidation peak between +0.61 and +0.65 V, which is attributed to the oxidation of the Cl^- anion. In addition, all the PS display a quasi-reversible peak between +0.87 and + 0.89 V, which is assigned to the oxidation of Ir^{III} core. In the cathodic region all the complexes feature an irreversible peak between -2.28 and -2.41 V ascribed to a ligand centered (**L1**-**L4**) reduction.[26,27] From the redox potentials and the E_{em} values (obtained from λ_{em}) we calculated the redox potential for the reductive and oxidative quenching in order to validate a possible redox mechanism for the photocatalytic activity of **[1]Cl**-**[4]Cl**.

6. Photostability of complexes [1]Cl and [3]Cl

The photostability of complexes **[1]Cl** and **[3]Cl** in solutions of both CD_3CN and $[D_6]DMSO/D_2O$ (3:2) ($1.4\cdot10^{-2}$ M), was studied by ^1H NMR over a period of 24 h under irradiation (LED blue light, λ_{irr} = 460 nm, 24 W) in a NMR tube exposed to atmospheric air. Complex **[1]Cl** exhibits an acceptable photostability in both solvent systems, with decomposition values of 13 % and 8% respectively, after 24 h. However, the species resulting from degration have not been identified (see ^1H NMR spectra in Figures SI12 and S13). Complex **[3]Cl** is also sufficiently stable in the mixture of solvents $[D_6]DMSO/D_2O$ (3:2), though decomposes slowly by dissociation of the N^N ligand (2% and 21% after 3 h and 24 h, respectively; see spectra in Figure SI15). On the contrary, **[3]Cl** is highly photosensitive in CD_3CN showing 96 % degradation after 24 h (Figure SI14). On the other hand, equivalent solutions of **[3]Cl** are stable in the dark at least after 2 weeks (Figure SI16).

7. Photooxidation of sulfides

Renaud et al. have previously reported on the photocatalytic activity of complex **[1]PF_6** in the aza-Henry reaction between N-phenyl tetrahydroisoquinoline and nitromethane under blue LED irradiation.[42] Inspired by this work and others,[16] we performed preliminary catalytic experiments on the photooxidation of thioanisole (**1a**) to methyl phenyl sulfoxide (**2a**) in the presence of **[1]Cl** at room temperature, under an O_2 atmosphere and with blue LED irradiation in different solvents (Table SI9). As a result, we concluded that the reaction was only feasible in protic solvents, such as MeOH and the mixture $DMSO/D_2O$ (3:2) and we chose the latter as the most beneficial in terms of conversion. This fact suggests a $^1O_2$ pathway.[9] Next, we carried out a catalysts screening, using **[1]Cl**-**[4]Cl** (0.1 mol %) as PSs, for the above-mentioned oxidation in a mixture of $[D_6]DMSO/D_2O$ (3:2) under the same conditions. This model transformation proceeds smoothly in the presence of the Ir^{III} PSs to give moderate or good yields after 12 h, and close to quantitative conversions after 18 h (entries 9-12 in Table 5). Interestingly, the catalytic activities determined by ^1H NMR for the different PSs were very similar, though benzylation seems to improve slightly the oxidation rate.

Table 5. Catalyst screening and control experiments in the photooxidation of thioanisole (**1a**) under an O_2 atmosphere and blue-LED irradiation (λ = 460 nm).[a]

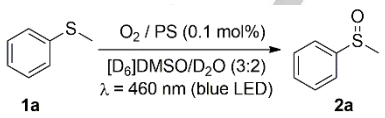

1a **2a**

Entry	Compound	Conditions	Conv. (%)[b]
1	**[1]Cl**	O_2, Dark	0
2	-	O_2, light	1
3	**[1]Cl**	N_2, light	0
4	**[1]Cl**	O_2,light, NaN_3[c]	<1
5	**[1]Cl**	O_2,light, 1,4-benzoquinone[d]	30
6	**[1]Cl**	O_2,light, 1,4-dimethoxybenzene[d]	15
7	$[Ir(C^N)_2(DMSO)Cl]$[f]	O_2, light	<1
8	$[Ir(C^N)_2(DMSO)Cl]$[f] + **L3**	O_2, light	<1
9	**[1]Cl**	O_2, light	59 (80)[e]
10	**[2]Cl**	O_2, light	64 (92)[e]
11	**[3]Cl**	O_2, light	67 (>99)[e]
12	**[4]Cl**	O_2, light	66 (82)[e]

[a] Thioanisole (**1a**) (10 mM), PS (10^{-2} mM, 0.1 mol %) in a mixture of $[D_6]DMSO/D_2O$ (0.5 mL, 3:2) at room temperature, under a saturated atmosphere of either O_2 or N_2 and under irradiation with blue light (LED, λ = 460 nm, 24 W) during 12 h in a septum-capped tube. [b] Conversion yields were determined by ^1H NMR analysis of the crude mixture as average values of two independent experiments. Overoxidation to the corresponding sulfone product was not detected in any experiment. [c] NaN_3 (11 mM). [d] Benzoquinone or 1,4 dimetoxybenzene (11 mM) [e] 18 h of irradiation. [f] Species formed from $[Ir(\mu\text{-}Cl)(C^N)_2]_2$ in DMSO containing solutions.

Moreover, the reaction is chemoselective, since no traces of over-oxidation products (sulfones) have been detected. The control experiments in the dark, in the absence of PS or in a N_2 atmosphere were unproductive (see entries 1-3 in Table 5), and the tests carried out in the presence of the free ligands as PSs were also sterile (see Table SI10). Besides, the use of either the Ir^{III} dimer, $[Ir(\mu\text{-}Cl)(C^N)_2]_2$ (which evolves *in situ* to $[Ir(C^N)_2(DMSO)Cl]$ in DMSO solutions) or a mixture of this precursor and **L3** as potential PSs only yielded traces of sulfoxide **2a** (entries 7 and 8 in Table 5). Hence, even though **[3]Cl** decomposes slightly into $[Ir(C^N)_2(DMSO)Cl]$ and **L3** in $[D_6]DMSO/D_2O$, these species do not contribute to the observed photocatalytic activity. In view of the above results, the photosensitizing role of the new Ir^{III} complexes is clearly established. Additional experiments were performed to

determine the actual oxidant and formulate a plausible mechanism. In particular, the addition of NaN_3 ($^1O_2$ quencher, entry 4 in Table 5) drastically suppressed the photooxidation of the substrate suggesting that the process is essentially mediated by $^1O_2$ in an energy transfer process (ET).[2],[43],[44].

Table 6. Photooxidation of sulphides **1** with **[3]Cl** under an O_2 atmosphere and blue-LED irradiation (λ = 460 nm).[a]

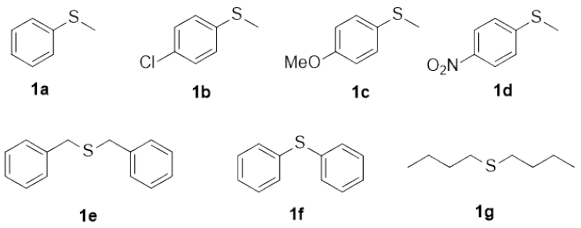

Entry	Compound	Conditions	Conv. (%)[b]
1	**1a**	O_2, light	67, >99[c][d]
2		air, light[c]	58, >99[c]
3	**1b**	O_2, light	46, >99[c]
4		air, light[d]	17, 53[c]
5	**1c**	O_2, light	53, >99[c]
6		air, light[d]	31, >99[c]
7	**1d**	O_2, light	19, 29[c]
8		air, light[d]	14[c]
9	**1e**	O_2, light	72, >99[c]
10		air, light[d]	38, >99[c]
11	**1f**	O_2, light	9, 44[c]
12		air, light[d]	9, 43[c]
13	**1g**	O_2, light	>99, >99[c]
14		air, light[d]	>99, >99[c]

[a] Sulphide (10 mM), **[3]Cl** (10^{-2} mM, 0.1 mol %) in a mixture of $[D_6]$DMSO/D_2O (0.5 mL, 3:2) at room temperature, under a saturated atmosphere of O_2 and under irradiation with blue light (LED, λ = 460 nm, 24 W) during 12 h in a septum-capped tube. [b] Conversion yields were determined by ^{1}H NMR analysis of the crude mixtures as average values of two independent experiments. Overoxidation to the corresponding sulfone product was not detected in any experiment. [c] **[3]Cl=** 1 mol %. [d] Reaction carried out in an open test tube.[d] Results previously described in Table 5 (entry 9) and inserted for comparation.

Other additives such as 1,4-benzoquinone (quencher of $O_2^{\bullet-}$) and 1,4-dimethoxybenzene (quencher of sulfide radical cations, $R_2S^{\bullet+}$)[16] (entries 5 and 6 in Table 5) were also used as indirect probes for $O_2^{\bullet-}$ and $R_2S^{\bullet+}$. Both scavengers gave rise to a partial decrease in the production of **2a** in agreement with a small contribution of an electron transfer (eT) pathway, in which the real oxidant is $O_2^{\bullet-}$ and where $R_2S^{\bullet+}$ are proposed as intermediates. All in all, the experimental data insinuate a dual mechanism. See the discussion below and Scheme 3 for more details.

To scrutinize the substrate scope of this methodology, the most active PS, **[3]Cl**, was selected to photocatalyze the oxidation of different sulphides (**1b-1g**) under an O_2 atmosphere. The results are summarized in Table 6 and the respective control experiments are compiled in Table SI11. Photoactivation of complex **[3]Cl** (0.1 mol %) catalyzed the oxidation of 4-Cl-thioanisole (**1b**), 4-OMe-thioanisole (**1c**), and dibenzylsulphide (**1e**) with moderate conversions after 12 hours, (46 to 72%) (entries 3, 5 and 9 in Table 6, respectively), whereas the dialkyl sulphide (**1g**) underwent complete transformation to the corresponding sulfoxide (entry 13, Table 6). On the contrary, diphenylsulphide (**1f**) was less prone to photooxidation (9 % conv.; entry 11 in Table 6).

Moreover, the photosensitized oxidation of all the above-mentioned substrates was also tested using atmospheric oxygen (air) instead of pure O_2 in the presence of **[3]Cl** at the same catalyst loading (0.1 mol %). Under these conditions the conversion values decreased notably for most of the sulphides (see entries 2, 4, 6, 10 and 12 in Table 6). Increasing the catalyst loading to 1 mol %, sulphides **1a**, **1c** and **1e** were oxidized to the corresponding sulfoxides with excellent conversions (>99%) under either pure O_2 or atmospheric O_2 (see entries 1-2, 5-6, and 9-10 in Table 6, respectively). Even the oxidation of **1f** was enhanced until 44 % conv. with this catalyst loading (see entries 11 and 12 in Table 6). The reluctant reaction of diaryl-sulphides with $^1O_2$ as compared to arylalkyl- and dialkyl-sulphides has been previously reported and could be related to the electrophilic nature of singlet oxygen.[45–47] In other words, $^1O_2$ possesses a low-energy LUMO (π_y*), compared to $^3O_2$, and hence it reacts more readily with sulphides having electron rich S atoms (alkyl sulphides) to form relatively stable persulfoxide intermediates (see mechanism in Scheme 3).

Substrate 4-nitrothioanisole (**1d**) is very singular and the results obtained in the corresponding photooxidation experiments deserve a detailed discussion. First of all, the yield for this sulphide in the presence of **[3]Cl** is very low (see entries 7 and 8 in Table 6). This fact could be attributed to a combination of different effects reported in the literature: (a) the electron-withdrawing nature of the nitro group that decreases the nucleophilic character of the S atom and makes **1d** less prone to photooxidation by electrophilic $^1O_2$;[9] (b) the ability of nitro compounds to deactivate excited states of PSs that could lead to quenching of the T_1 state of **[3]Cl** by **1d**;[48] (c) the ability of trapping radicals attributed to the nitro group,[2] which could inhibit the eT pathway in the photooxidation of **1d**. In the second place, the yield for **1d** in the absence of PS is surprisingly high (15%, entry 7 in Table SI11). Indeed, the self-induced photooxidation of 4-nitrophenyl alkyl sulphides has been previously described and explained as a consequence of their capability of sensitizing the conversion of $^3O_2$ to $^1O_2$.[49]

We have done additional photocatalytic assays for **1a** with **[1]Cl** in DMSO/H_2O (3:2) and $[D_6]$DMSO/D_2O (3:2) (See Table SI9).

Thus, the oxidation rate with **[1]Cl** is higher using deuterated solvents, in agreement with its longer $\tau_{1/2}$ in [D_6]DMSO/D_2O (3:2) versus DMSO/H_2O (3:2) (Table 4), which suggests a main pathway mediated by $^1O_2$.[2] We postulate that the presence of the N-H group in **[1]Cl** facilitates the interaction between the excited state of the PS and protic solvents as well as H or D exchange leading to faster quenching in non-deuterated solvents. Analogous experiments with **[3]Cl** in DMSO/H_2O (3:2) (Table SI12) and [D_6]DMSO/D_2O (3:2) (Table 6) gave similar conversion values in line with the comparable $\tau_{1/2}$ values obtained in both solvent systems for **[3]Cl**, which proves the absence of isotopic effects for this PS in accordance with the lack of functional groups able to interact efficiently with protic solvents.

In order to demonstrate that other sources of light can be used in this transformation, photocatalytic experiments with a CFL lamp have been done, using complex **[3]Cl** as the catalyst (0.1 mol% and 1 mol%) in [D_6]DMSO/D_2O (3:2) (see Table SI13). The results are similar to those obtained with the blue LED light.

8. Photooxidation of sulfur containing *L*-Aminoacids.

Next, we decided to test the potential of complexes **[1]Cl** and **[3]Cl** in the photooxidation of the sulfur-containing aminoacids, *L*-cysteine and *L*-methionine. The results collected in Table 7 demonstrate that the new PSs are active in the chemoselective oxidation of both *L*-aminoacids to cystine and methionine sulfoxide, respectively (^{1}H NMR spectra in Figures SI24 and SI25). Again, the control experiments confirm the active role of the Ir^{III} derivatives (see entries 1 and 4 in Table 7).

Table 7. Photo-oxidation of *L*-methionine or *L*-cysteine under an O_2 atmosphere and blue-LED irradiation.[a]

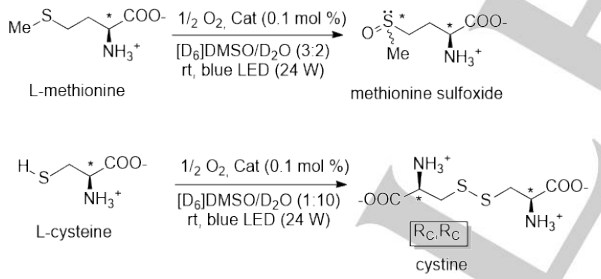

Entry	Compound	Substrate	Conditions	Conv. (%)[b]
1	-	**L-Met**	O_2, light	0
2	**[1]Cl**	**L-Met**	O_2, light	62, 95[c]
3	**[3]Cl**	**L-Met**	O_2, light	75, 99[c]
4	-	**L-Cys**	O_2, light	44
5	**[1]Cl**	**L-Cys**	O_2, light	>99
6	**[3]Cl**	**L-Cys**	O_2, light	>99

[a] *L*-methionine/*L*-cysteine (10 mM), PS (10^{-2} mM, 0.1 mol %) in a mixture of [D6]DMSO/D_2O (0.5 mL, 3:2 or 1:10 respectively) at room temperature, under a saturated atmosphere of O_2 and under irradiation with blue light (LED,λ = 460 nm, 24 W) in a septum-capped tube. [b] Conversion yields were determined by ^{1}H NMR analysis of the crude mixture as average values of two independent experiments. ESI-MS spectra were recorded to confirm the identity of products. Methionine sulfoxide was obtained as a 1:1 mixture of diastereoisomers which are epimers at the sulfur atom, that is (S_S,S_C) and (R_S,S_C) and Cystine was obtained as the (R,R) diastereomer. Overoxidation to methionine sulfone or cysteine sulfenic, sulfinic or sulfonic acids was not detected in any experiment. A turbid suspension attributed to cystine precipitation was observed after stopping the reaction with L-cysteine, which was acidified to dissolved it. [c] 18 h of irradiation.

9. Mechanistic proposal

On the basis of our experimental observations (see Table 8) and the bibliographic background,[2][50,51] we tentatively propose a dual mechanism for the photosensitized oxidation of sulphides under O_2 atmosphere in the presence of complexes **[1]Cl-[4]Cl** as photosensitizers (

Scheme *3*): this involves an ET pathway mediated by $^1O_2$ (see Scheme 3a) and a concurrent eT pathway mediated by $O_2^{\bullet-}$ (see Scheme 3b).

Table 8. Experimental observations with mechanistic implications.

Pathway	Evidences
ET ($^1O_2$)	• Exp. with NaN_3 ($^1O_2$) unproductive (Table 5). • Low conv. for diphenylsulphide (**1f**) (Table 6). • Low conv. for 4-nitrothioanisole (**1d**) (Table 6). • Protic solvents promote oxidation of **1a** (Table SI8). • Higher conv. for **[1]Cl** in deuterated solv. (Table SI8).
eT ($O_2^{\bullet-}$)	• Low conv. with 1,4-benzoquinone (Table 5). • Low conv. with 1,4-dimetoxybenzene (Table 5). • Electrochemical experiments.
$^1O_2 \rightarrow O_2^{\bullet-}$ Step	• Exp. with NaN_3 ($^1O_2$) unproductive (Table 5).

The ET route starts with the photosensitization of $^3O_2$ to $^1O_2$ in three steps: (a) the Ir^{III} photosensitizer [Ir^{III}] is excited with visible light from the ground state (S_0) to higher energy singlet states (S_n), which undergo partial relaxation to the lowest energy excited singlet state, S_1, (^{1}[Ir^{III}]*); (b) next, the Ir-PS may go through an intersystem crossing process from the S_1 state to the lowest energy excited triplet state, T_1, (^{3}[Ir^{III}]*); (c) subsequently, $^3O_2$ quenches the ^{3}[Ir^{III}]* via an energy transfer (ET) process to produce $^1O_2$. The electronic configuration of $^1O_2$($^1\Delta_g$) bestows an electrophilic character to this excited state of dioxygen that facilitates the oxidation of nucleophiles, such as sulphides.[51] Therefore, singlet oxygen $^1O_2$($^1\Delta_g$) reacts with the corresponding sulphide generating the persulfoxide intermediate, **A**, which in turn reacts with other molecule of sulphide to produce two molecules of the respective sulfoxide.[52]

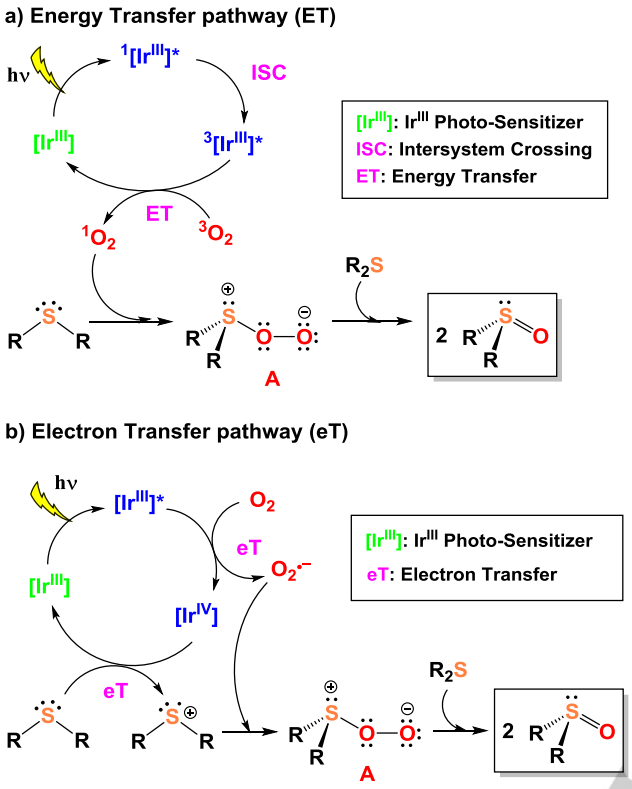

Scheme 3. Dual mechanistic proposal for the photocatalytic oxidation of sulphides. a) photooxidation mediated by $^1O_2$ (ET pathway); b) photooxidation mediated by $O_2^{\bullet-}$ (eT pathway).

Alternatively, the photooxidation can occur through an eT pathway. In this case, the highly reductive Ir^{III} excited species, $[Ir^{III}]^*$ ($E^o(Ir^{IV}/Ir^{III*})$ = -1.71 V, see Scheme SI1) can reduce a molecule of O_2 to generate the superoxide radical ($O_2^{\bullet-}$) and concurrently the intermediate $[Ir^{IV}]$ through oxidative quenching. Next, the $[Ir^{IV}]$ intermediate ($E^o(Ir^{IV}/Ir^{III})$ = + 0.87 V) can oxidize a molecule of sulphide to generate a sulphide radical cation, $R_2S^{\bullet+}$ ($E^o(R_2S^{\bullet+}/R_2S)$ = +1.02 V, experimentally measured for thioanisol by CV) and concomitantly regenerate the $[Ir^{III}]$ PS. This step is plausible, though the process is slightly endergonic (ΔE^o = -0.15 V), in as much as $R_2S^{\bullet+}$ reacts and transforms quickly in a different species.[53] Indeed, we propose that the superoxide ($O_2^{\bullet-}$) reacts with $R_2S^{\bullet+}$ to produce the corresponding persulfoxide, **A**, and finally the sulfoxide, upon the intervention of another molecule of sulphide. However, taking into account the almost complete inhibition of the reaction in the presence of NaN_3 (entry 4, Table 5), we speculate that NaN_3 (strong reducing agent) can interfere with this pathway by reducing $[Ir^{IV}]$ to $[Ir^{III}]$.

Conclusions

In conclusion, we have synthesised and fully characterized a new family of Ir^{III} complexes of general formula $[Ir(ppy)_2(N^N)]Cl$, where N^N stands for either 2,2'-bipyridylamine (**L1**) or its benzylated derivatives (**L2-L4**). The new compounds exhibit photoluminescent properties and remarkable photocatalytic activity in the aerobic oxidation of organic sulphides. In particular, **[3]Cl** was identified as the most active PS in the O_2-mediated photooxidation of thioanisole and exhibited excellent performances in the selective achievement of different dialkyl, alkylaryl and diaryl sulfoxides from their respective sulphides. Likewise, the oxidation of S-containing *L*-aminoacids was selectively accomplished under similar conditions. By-products or over-oxidation products were not detected in any case. Moreover, the catalytic transformations proceeded in a mixture of DMSO/H_2O at room temperature, with low catalyst loading and in the absence of additives or sacrificial oxidants. Indeed, the experimental data suggest that both $^1O_2$ and $O_2^{\bullet-}$ contribute as the actual oxidant agents in alternative pathways. To the best of our knowledge, systematic studies on the photooxidation of sulphides using Ir^{III} complexes as PSs have not been described previously and so, this contribution could open a new line of work for Ir-based photocatalysis. To conclude, future developments in this area should focus on the design of new PSs to improve both their photostability and their absorption properties.

Experimental Section

General experimental procedure for the synthesis of ligands L2-L4

In a 100 mL Schlenk flask, previously purged with nitrogen, N,N-dipyridylamine (dpa, **L1,** 2.34 mmol) was added to a suspension of powdered KOH (9.45 mmol) in DMSO (4 mL) and the mixture was stirred for 40 min to facilitate the deprotonation of dpa (**L1**). Then, the appropriate benzyl bromide (2.34 mmol) was added, and the reaction mixture was stirred at room temperature for 24 h. Addition of water (5 mL) followed by fridge cooling (24 h) gave rise to precipitation of the crude ligand which was collected by filtration, washed with water (3 x 5 mL) and dried under vacuum. The resulting products were recrystallized in n-hexane to produce the desired pure ligands.

General experimental procedure for the synthesis of complexes [1]Cl-[4]Cl

In a 100 mL Schlenk flask, previously purged with nitrogen, the N^N ligand **L1-L4** (0.18 mmol) was added to a solution of $[Ir(\mu\text{-}Cl)(C^N)_2]_2$ (0.100 g, 0.09 mmol) in a mixture of dichloromethane (10 mL) and methanol (5 mL). The resulting solution was stirred at 50 °C for 6 h under a nitrogen atmosphere. Diethyl ether or *n*-hexane (20 mL) was added to precipitate a crude solid, which was filtered and washed with diethyl ether (2×10 mL). The solid was dried under vacuum.

X-ray Crystallography.

A summary of crystal data collection and refinement parameters for **[1]Cl** are given in Table SI3. A single crystal of **[1]Cl** was coated in high-

vacuum grease, mounted on a glass fiber and transferred to a Bruker SMART APEX CCD-based diffractometer equipped with a graphite monochromated Mo-Kα radiation source (λ = 0.71073 Å). The highly redundant datasets were integrated using SAINT[54] and corrected for Lorentz and polarization effects. The absorption correction was based on the function fitting to the empirical transmission surface as sampled by multiple equivalent measurements with the program SADABS.[55] The software package WINGX[56] was used for space group determination, structure solution, and refinement by full-matrix least-squares methods based on F^2. A successful solution by direct methods provided most non-hydrogen atoms from the E-map. The remaining non-hydrogen atoms were located in an alternating series of least-squares cycles and difference Fourier maps. All non-hydrogen atoms were refined with anisotropic displacement coefficients. Hydrogen atoms were placed using a "riding model" and included in the refinement at calculated positions. CCDC reference number for **[1]Cl** is 1825414.

Electrochemical measurements

Electrochemical measurements were performed using a portable Bipotentiostat μSTAT 300 (DropSens) equipment controlled by DropView (DropSens). All experiments were carried out using a three-electrode cell using a glassy-carbon disk with a diameter of 3 mm as the working electrode, a platinum wire as the auxiliary electrode, and a RE-5B Ag/AgCl (BASi) reference electrode. Oxygen was removed from the solution by bubbling argon for 10 min and keeping the argon atmosphere along the whole experiment. The formal potentials were determined by cyclic voltammetry (CV), at a scan rate of 100 mV s^{-1}. All potentials were referred to ferrocene as internal standard. All voltammetric experiments were started and finished at a potential of −0.46 V and performed in a clockwise direction. Acetonitrile solutions of the complexes (10^{-3} M) were used in the presence of 0.1 M [^{n}Bu$_4$N][PF$_6$] as supporting electrolyte.

General procedure for photocatalytic oxidation

In a septum-capped tube we added the corresponding sulphide or *L*-aminoacid (5 μmol in solution of [D$_6$]DMSO), the Ir(III) catalyst **[1]Cl-[4]Cl** (0.005 or 0.05 μmol in solution of [D$_6$]DMSO), and additional DMSO and D_2O, obtaining the mixture [D$_6$]DMSO/D_2O (0.5 mL; 3:2 v/v) and providing the desired final concentration of substrate, 10 mM. The system was purged with O_2 or N_2 until atmosphere saturation and irradiated with Blue LED light (λ= 460 nm, 24W) or CFL lamp at room temperature during 12 h. The yield values for sulfoxides were calculated by ^{1}H NMR integration from the crude mixture when the reaction was done in deuterated solvents. Alternatively, when the reactions were performed in non-deuterated solvents an aliquot of the crude solution (100 μL) was added to 400 μL of [D$_6$]DMSO, and the yield values for sulfoxides were calculated by ^{1}H NMR integration.

Acknowledgements

Dr. M. Vaquero is grateful for the financial support received from the Consejería de Educación-Junta de Castilla y León (BU042U16).
Financial support by the Spanish Ministry of Economy and Competitiveness (MINECO) (projects CTQ2014-58812-C2-1-R, (CTQ2014-58812-C2-2-R, CTQ2015-70371-REDT, FEDER funds), Obra Social "la Caixa" (OSLC-2012-007), Junta de Castilla y León (BU-042U16), is gratefully acknowledged. We are also indebted to P. Castroviejo and M. Mansilla, from PCI of the University of Burgos, for technical support.

Keywords: Biscyclometalated Iridium(III) Complexes • Oxygen photosensitizers • Photocatalysis • Singlet Oxygen • Sulphides photooxidation.

[1] J. Twilton, C. C. (Chip) Le, P. Zhang, M. H. Shaw, R. W. Evans, D. W. C. MacMillan, *Nat. Rev. Chem.* **2017**, *1*, 52.
[2] T. Neveselý, E. Svobodová, J. Chudoba, M. Sikorski, R. Cibulka, *Adv. Synth. Catal.* **2016**, *358*, 1654–1663.
[3] M. H. Shaw, J. Twilton, D. W. C. MacMillan, *J. Org. Chem.* **2016**, *81*, 6898–6926.
[4] L. Huang, J. Zhao, S. Guo, C. Zhang, J. Ma, *J. Org. Chem.* **2013**, *78*, 5627–5637.
[5] M. S. Baptista, J. Cadet, P. Di Mascio, A. A. Ghogare, A. Greer, M. R. Hamblin, C. Lorente, S. C. Nunez, M. S. Ribeiro, A. H. Thomas, et al., *Photochem. Photobiol.* **2017**, *93*, 912–919.
[6] N. Iqbal, S. Choi, Y. You, E. J. Cho, *Tetrahedron Lett.* **2013**, *54*, 6222–6225.
[7] T. L. Lam, J. Lai, R. R. Annapureddy, M. Xue, C. Yang, Y. Guan, P. Zhou, S. L.-F. Chan, *Inorg. Chem.* **2017**, *56*, 10835–10839.
[8] O. Hamelin, P. Guillo, F. Loiseau, M. F. Boissonnet, S. Ménage, *Inorg. Chem.* **2011**, *50*, 7952–7954.
[9] J. Dad'ová, E. Svobodová, M. Sikorski, B. König, R. Cibulka, *ChemCatChem* **2012**, *4*, 620–623.
[10] B. Kasprzyk-Hordern, *Chem. Soc. Rev.* **2010**, *39*, 4466.
[11] A. Guerrero-Corella, A. María Martinez-Gualda, F. Ahmadi, E. Ming, A. Fraile, J. Alemán, *Chem. Commun.* **2017**, *53*, 10463–10466.
[12] I. Fernández, N. Khiar, *Chem. Rev.* **2003**, *103*, 3651–3705.
[13] J. Legros, J. R. Dehli, C. Bolm, *Adv. Synth. Catal.* **2005**, *347*, 19–31.
[14] X. Gu, X. Li, Y. Chai, Q. Yang, P. Li, Y. Yao, *Green Chem.* **2013**, *15*, 357.
[15] C. Ye, Y. Zhang, A. Ding, Y. Hu, H. Guo, *Sci. Rep.* **2018**, *8*, 2205.
[16] A. Casado-Sánchez, R. Gómez-Ballesteros, F. Tato, F. J. Soriano, G. Pascual-Coca, S. Cabrera, J. Alemán, *Chem. Commun.* **2016**, *52*, 9137–9140.
[17] D. Chao, M. Zhao, *ChemSusChem* **2017**, *10*, 3358–3362.
[18] H.-J. Xu, Y.-C. Lin, X. Wan, C.-Y. Yang, Y.-S. Feng, *Tetrahedron* **2010**, *66*, 8823–8827.
[19] W. Li, Z. Xie, X. Jing, *Catal. Commun.* **2011**, *16*, 94–97.
[20] A. Hassan, S. R. Breeze, S. Courtenay, C. Deslippe, S. Wang, *Organometallics* **1996**, *15*, 5613–5621.
[21] S. Fakih, W. C. Tung, D. Eierhoff, C. Mock, B. Krebs, *Zeitschrift für Anorg. und Allg. Chemie* **2005**, *631*, 1397–1402.
[22] B. Antonioli, D. J. Bray, J. K. Clegg, K. Gloe, K. Gloe, O. Kataeva, L. F. Lindoy, J. C. McMurtrie, P. J. Steel, C. J. Sumby, et al., *Dalton Trans.* **2006**, 4783–4794.
[23] A. J. Swarts, S. F. Mapolie, *Dalton Trans.* **2014**, *43*, 9892–9900.
[24] A. J. Swarts, F. Zheng, V. J. Smith, E. Nordlander, S. F. Mapolie, *Organometallics* **2014**, *33*, 2247–2256.
[25] S. Sprouse, K. A. King, P. J. Spellane, R. J. Watts, *J. Am. Chem. Soc.* **1984**, *106*, 6647–6653.
[26] M. C. Tseng, W. L. Su, Y. C. Yu, S. P. Wang, W. L. Huang, *Inorganica Chim. Acta* **2006**, *359*, 4144–4148.
[27] M. Martínez-Alonso, J. Cerdá, C. Momblona, A. Pertegás, J. M. Junquera-Hernández, A. Heras, A. M. Rodríguez, G. Espino, H. Bolink, E. Ortí, *Inorg. Chem.* **2017**, *56*, 10298–10310.
[28] E. Baranoff, B. F. E. Curchod, J. Frey, R. Scopelliti, F. Kessler, I. Tavernelli, U. Rothlisberger, M. Grätzel, M. K. Nazeeruddin, M. Gratzel, et al., *Inorg. Chem.* **2012**, *51*, 215–224.
[29] K. S. Bejoymohandas, T. M. George, S. Bhattacharya, S. Natarajan, M. L. P. Reddy, *J. Mater. Chem. C* **2014**, *2*, 515–523.
[30] H. Sun, S. Liu, W. Lin, K. Y. Zhang, W. Lv, X. Huang, F. Huo, H. Yang, G. Jenkins, Q. Zhao, et al., *Nat. Commun.* **2014**, *5*, 3601.
[31] G. E. Schneider, H. J. Bolink, E. C. Constable, C. D. Ertl, C. E. Housecroft, A. Pertegas, J. A. Zampese, A. Kanitz, F. Kessler, S. B. Meier, *Dalton Trans.* **2014**, *43*, 1961–1964.
[32] A. Maity, L. Q. Le, Z. Zhu, J. Bao, T. S. Teets, *Inorg. Chem.* **2016**, *55*, 2299–2308.
[33] E. Baranoff, B. F. E. Curchod, *Dalton Trans.* **2015**, *44*, 8318–8329.
[34] W. Lin, Q. Zhao, H. Sun, K. Y. Zhang, H. Yang, Q. Yu, X. Zhou, S. Guo, S. Liu, W. Huang, *Adv. Opt. Mater.* **2015**, *3*, 368–375.
[35] H. Cao, H. Sun, Y. Yin, X. Wen, G. Shan, Z. Su, R. Zhong, W. Xie, P. Li, D. Zhu, *J. Mater. Chem. C* **2014**, *2*, 2150–2159.
[36] G. E. Schneider, A. Pertegás, E. C. Constable, C. E. Housecroft, N.

Hostettler, C. D. Morris, J. A. Zampese, H. J. Bolink, J. M. Junquera-Hernández, E. Ortí, et al., *J. Mater. Chem. C* **2014**, *2*, 7047.
[37] S. Meng, I. Jung, J. Feng, R. Scopelliti, D. Di Censo, M. Grätzel, M. K. Nazeeruddin, E. Baranoff, *Eur. J. Inorg. Chem.* **2012**, *2012*, 3209–3215.
[38] V. Russell, M. Scudder, I. Dance, *J. Chem. Soc. Dalton Trans.* **2001**, 789–799.
[39] I. Dance, M. Scudder, *CrystEngComm* **2009**, *11*, 2233.
[40] R. D. Costa, E. Ortí, H. J. Bolink, F. Monti, G. Accorsi, N. Armaroli, *Angew. Chemie - Int. Ed.* **2012**, *51*, 8178–8211.
[41] S. Chen, R. Fan, X. Wang, Y. Yang, *Inorg. Chem. Commun.* **2014**, *44*, 101–106.
[42] E. Sauvageot, R. Marion, F. Sguerra, A. Grimault, R. Daniellou, M. Hamel, S. Gaillard, J.-L. Renaud, *Org. Chem. Front.* **2014**, *1*, 639–644.
[43] A. Kando, Y. Hisamatsu, H. Ohwada, T. Itoh, S. Moromizato, M. Kohno, S. Aoki, *Inorg. Chem.* **2015**, *54*, 5342–5357.
[44] A. Nakagawa, Y. Hisamatsu, S. Moromizato, M. Kohno, S. Aoki, *Inorg. Chem.* **2014**, *53*, 409–422.
[45] F. Jensen, A. Greer, E. L. Clennan, *J. Am. Chem. Soc.* **1998**, *120*, 4439–4449.
[46] C. S. Foote, J. W. Peters, *J. Am. Chem. Soc.* **1971**, *93*, 3795–3796.
[47] K. L. Stensaas, B. V. McCarty, N. M. Touchette, J. B. Brock, *Tetrahedron* **2006**, *62*, 10683–10687.
[48] G. R. Seely, *J. Phys. Chem.* **1969**, *73*, 125–129.
[49] D. J. Pasto, F. Cottard, L. Jumelle, *J. Am. Chem. Soc.* **1994**, *116*, 8978–8984.
[50] E. L. Clennan, *The Reactions of Sulfides and Sulfenic Acid Derivatives with Singlet Oxygen*, **1996**.
[51] M. C. DeRosa, R. J. Crutchley, *Coord. Chem. Rev.* **2002**, *234*, 351–371.
[52] J. J. Liang, C. L. Gu, M. L. Kacher, C. S. Foote, *J. Am. Chem. Soc.* **1983**, *105*, 4717–4721.
[53] D. Astruc, *Electron Transfer and Radical Processes in Transition-Metal Chemistry*, Wiley-VCH, **1995**.
[54] B. N. Axs, *SAINT Area-Detector Integr. Program. SAINT+ v7.12a.; Madison, Wisconsin, USA* **2004**.
[55] G. M. Sheldrick, *SADABS A Progr. Empir. Absorpt. Correct. Version 2004/1; Univ. Göttingen, Göttingen, Ger.* **2004**.
[56] B.-N. Axs, *SHELXTL-NT Struct. Determ. Packag. Version 6.12.; Madison, Wisconsin, USA* **2001**.

10.1002/chem.201801173

WILEY-VCH

Entry for the Table of Contents (Please choose one layout)

Layout 1:

FULL PAPER

Selective and Efficient Ir^{III} Photosensitizers: Selective biscyclometalated Ir^{III} photosensitizers for the oxidation of sulphides under visible-light irradiation are described. Experimental observations support a dual mechanism where singlet oxygen and superoxide are the actual oxidants.

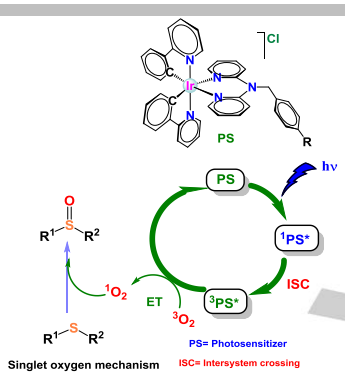

Mónica Vaquero, Alba Ruiz-Riaguas, Marta Martínez-Alonso, Félix A. Jalón, Blanca R. Manzano, Ana M. Rodríguez, Gabriel García-Herbosa, Arancha Carbayo, Begoña García, Gustavo Espino**

Page No. – Page No.
Selective Photooxidation of Sulphides catalyzed by Biscyclometalated Ir^{III} Photosensitizers Bearing 2,2'-dipyridylamine Based Ligands

Layout 2:

FULL PAPER

((Insert TOC Graphic here; max. width: 11.5 cm; max. height: 2.5 cm))

*Author(s), Corresponding Author(s)**

Page No. – Page No.

Title

Text for Table of Contents